Long-term behaviour of water vapour absorption in hollow core fibres

Shuichiro Rikimi[1*], Yong Chen[1,2], Thomas D. Bradley[1], Marcelo A. Gouveia[2], Ray Horley[2], Andrew Harker[2], Simon Bawn[2], Francesco Poletti[1], Marco N. Petrovich[1,2], David J. Richardson[1] and Natalie V. Wheeler[1]

[1]Optoelectronics Research Centre, University of Southampton, Southampton, United Kingdom
[2]Lumenisity Ltd, Unit 7, The Quadrangle, Premier Way, Romsey, United Kingdom

Abstract

We report on the long-term behaviour of water vapour absorption in 19 cell HC-PBGFs in open and spliced conditions. Two main trends were observed as a function of time: increase in absorption of water vapour after opening sealed ends and reduction of the absorption after splicing ends. Furthermore, attenuation at 1550 nm was not significantly influenced by water vapour dynamics at 22 ℃ and 85 ℃.

Keywords: hollow core fibre, optical fibre testing, gas sensing

* sr1y15@soton.ac.uk

I Introduction

Recent advances in hollow core fibre (HCF) fabrication[1] are driving increasing interest in these fibres for future applications in telecommunications, ultra-high power delivery and sensing. While guidance in a hollow core leads to the unique properties of HCFs, such as ultimate low latency, low nonlinearity and the potential for ultra-low loss, the gas content within the core and the surrounding microstructure has the potential to impact both the optical and mechanical properties of the fibre[2,3].

In several applications (usually requiring reasonably short fibre lengths), such as gas sensing and nonlinear optics[4,5], the gas content in the hollow core region is carefully controlled. However, in many other experiments, little attention is paid to the composition of the gas inside a HCF. This gas composition is likely to be largely ambient air and accordingly measurements have recorded the presence of nitrogen, oxygen, water vapour and carbon dioxide in HCFs[6,7]. Yet the gas composition is also influenced by the fibre fabrication process (the exact grade of silica glass used as the raw material, the fibre draw parameters and the gas used to control the hole size during fabrication), which can lead to the presence of additional gas species such as inert gasses and hydrogen chloride[2]. Finally, it will also be influenced by whether the HCF is used in a sealed condition (for example, spliced at both ends to conventional fibre for use in telecommunications) or with both ends open to the surrounding environment (as in several sensing configurations). Optically, absorption resonances from different gas species can increase the fibre attenuation in specific spectral regions. Furthermore, it is feasible that chemical reactions between gas species within the fibre or operation at very low temperatures could lead to increased scattering loss.

In this work, we focus on the effects of water vapour in HCFs. Water presents an especially complex behaviour as it can exist in the vapour phase and therefore be observed in transmission measurements but it also interacts with the silica glass membranes of the fibre. Previous work[8], reported in 2012, studied water ingress into a 50 m length of HCF over a period of 28 weeks and showed growth of a broadband spectral feature around 1398 nm which was attributed to the interaction with the silica surfaces within the fibre. Although water vapour absorption spectra were also shown, the development of these with time was not discussed.

Here, we describe optical measurements of water vapour absorption in HCFs over a range of time scales in both open and sealed conditions and at elevated temperatures. The absorption at 1369.85 nm varied with time in both of those

conditions and the temperature behaviour was observed. Furthermore, the attenuation was also recorded and it was found that loss at 1550 nm was not significantly influenced by water vapour dynamics at 22 ℃ and 85 ℃.

II Experimental setup and method

For this work, all the fibres used were 19-cell HC-PBGFs with a similar design to the fibre reported[9]. A typical cross-sectional image is shown in Fig. 1(c). The fibres were designed for operation around 1550 nm but also have low attenuation between 1350 nm and 1550 nm which overlaps with the $v_1 + v_3$ and $2v_1$ absorption bands of water vapour (HITRAN data Fig. 1(a), PBGF transmission Fig. 1(b)).

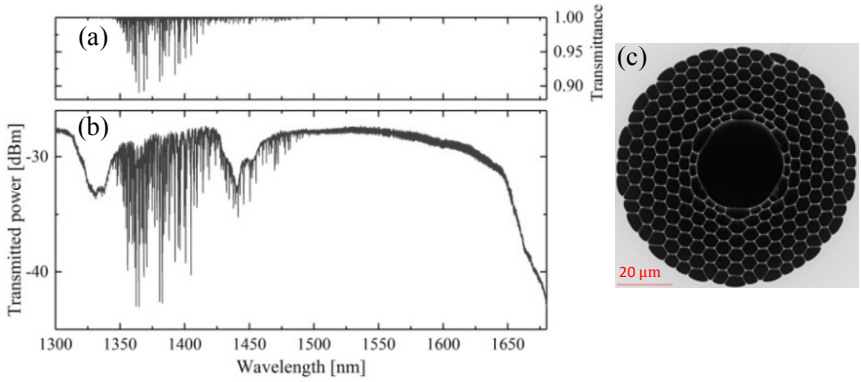

Fig. 1: (a) Transmittance of water vapour from HITRAN database (1 ppm, 1 km, 0.05 nm filter) (b) transmitted spectra recorded at 0.05 nm resolution and (c) scanning electron micrograph of PBGF-A (55 m).

1. Water vapour ingress into open HCFs

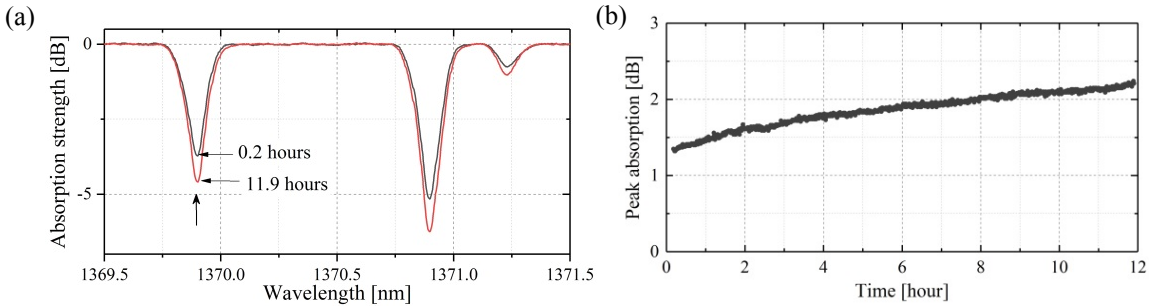

Fig. 2: (a) Evolution of spectral absorption of water vapour in 35 m of PBGF-A with time. The arrowed line is at 1369.85 nm. (b) Ingress of water vapour in PBGF-A; the sample was open to the atmosphere for 12 hours. The measurement time was started when the first fibre end was cleaved.

In this section the ingress of water vapour from the atmosphere is investigated. A 35 m length of HC-PBGF (PBGF-A) was kept in a laboratory with sealed ends prior to this experiment. The aim of the experiment was to measure the variation of water vapour absorption in the HCF immediately after opening the fibres to atmospheric conditions by cleaving both ends. For this measurement, a supercontinuum (SC) laser was used as a light source because high power spectral density was required to obtain high resolution measurements of the gas absorption lines. The transmitted power as a function of wavelength was recorded using an optical spectrum analyser (OSA) at 0.05 nm resolution. The SC light was launched into the HC-PBGF via a single mode fibre (SMF) and the output was collected by a SMF. A ~0.3 mm gap was set between the SMFs and the sample to allow atmospheric air access to the hollow core region. The laboratory relative humidity and temperature were 35.5 % and 24 ℃ for the duration of the test. In order to eliminate any contribution other than from the HC-PBGF assembly (e.g. water vapour in the free-space path within the SC laser and

the OSA), reference data was separately recorded and subtracted (Fig. 2(b)). Note, reference data was also collected for measurements presented later in Fig. 3(a) and 4.

The time variation of water vapour absorption between 1369.5 nm and 1371.5 nm in PBGF-A is shown in Fig. 2(a). In this paper we selected the absorption line at 1369.85 nm for detailed analysis of water vapour dynamics because it is a relatively isolated peak and has moderate absorption strength (excluding PBGF-C measurements where absorption at 1399.65 nm was monitored due to the limited transmission at 1369.85 nm).

Fig. 2(b) shows that the water vapour absorption strength at 1369.85 nm gradually increased for 12 hours after opening the ends in PBGF-A. It indicates that water vapour present in air diffused into the hollow core when the fibre was exposed to the atmosphere. The initial absorption at the start of the measurement is attributed to water vapour pre-existing in the HCF as well as water vapur that has previously ingressed. Further data (not shown) showed that the rate of increasing absorption and the initial level of water absorption varied between different HCF samples.

2. Water vapour absorption in sealed HCFs

In this section, the behaviour of water vapour in sealed HCFs is discussed. Two different HCFs (PBGF-B, length 625 m and PBGF-C, 498 m) were prepared by splicing them at both ends to SMFs via solid buffer fibres (BFs). The BFs were used to adjust the mode field diameter between the HC-PBGF and the SMF. During the splicing process, the fibres were open to the atmosphere for ~1 hour. After splices at both ends are applied, the HC-PBGFs become effectively hermetically sealed; in this condition, further atmospheric ingression is prevented and cannot impact the fibre's transmission properties.

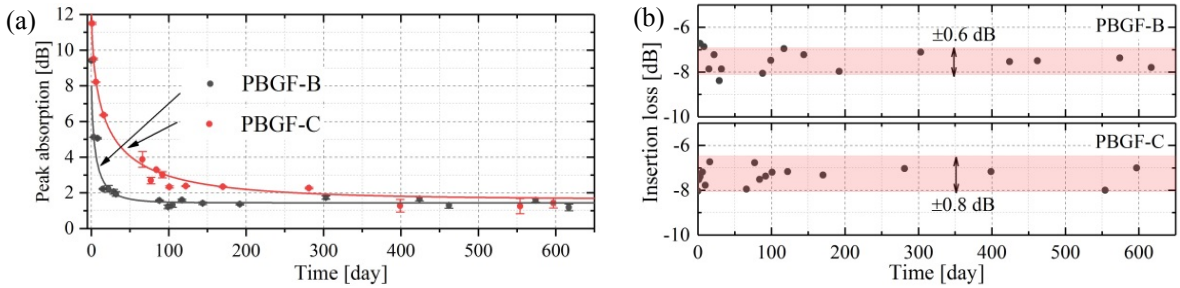

Fig 3: (a) Evolution of water vapour absorption strength with respect to time; black circle: PBGF-B at 1369.85 nm, red circle: PBGF-C at 1399.65 nm. (b) Insertion loss at 1550 nm at 10 nm resolution.

The two fibres showed similar trends over time and the results are shown in Fig. 3(a). The absorption by water vapour significantly decreases over a time period of ~14 days post-splicing. Following this, the observed absorption level continues to decrease, slowly approaching a stable state, but does not disappear even after 600 days. The decreasing trend is not a simple exponential decay; following previous work[10], the absorption strength, $P(t)$, can be described by

$$P(t) = A \times \exp\left(-\left(\frac{t}{\tau}\right)^{a}\right) + B. \qquad (1)$$

Here, τ is defined as the absorption decay time and a is a constant depending on the adsorption mechanics. A and B are the absorption strengths for the initial and equilibrium states, respectively. Fitting (1) to the experimental data in Fig. 3(a) gives 0.57 and 0.47 for a and 5.17 day and 18.6 day for τ in PBGF-B and PBGF-C, respectively.

In parallel, the transmitted power at 1550 nm through the samples was recorded. Fig. 3(b) shows the measured insertion loss of the HC-PBGFs (including the splice losses) as a function of time. The shaded areas represent the measurement uncertainty due to variable connection loss at the input which was separately measured by removing and reattaching the connectors. The standard deviation of the transmitted power due to the variable connection loss was ±

0.6 dB and ± 0.8 dB at 1550 nm for PBGF-B and PBGF-C respectively. Overall, no significant power change was observed with time within the measurement uncertainty.

Section 1 suggests that water vapour in the atmosphere is one of the sources of the water absorption post-splicing (day 0). This vapour can, through diffusion, move along the fibre length. The data in Fig. 3(a) shows that in a sealed condition, water vapour absorption decreases, indicating less water is in the light path. Possible scenarios which explain our result are that water molecules are sticking to silica surfaces within the HCF or chemically reacting with another gas species, such as hydrogen chloride, in the core. It is well known that water is a very reactive molecule with glass, both chemically and physically[8,11]. Water molecules that chemically react with silica can exist on the glass surface as a silanol (Si-OH) and can also physically be adsorbed. An OH-covered glass surface can capture further water vapour through hydrogen bonding ($SiOH\text{-}OH_2$) and thus there are possible reactions describing the interaction of the water molecules with the glass involving mono- and multiple layers.

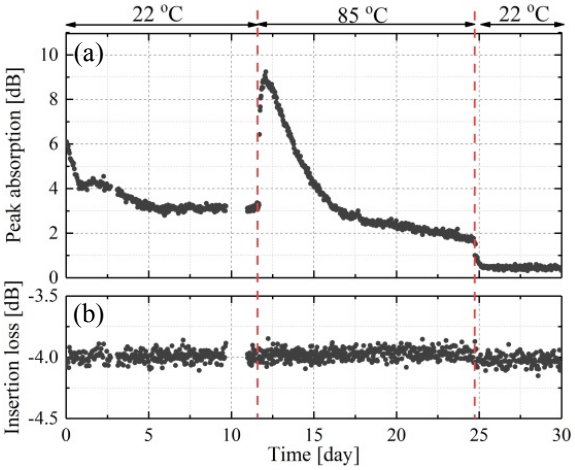

Fig 4: Variation of (a) water vapour absorption strength and (b) insertion loss at 1550 nm recorded at 2 nm resolution in PBGF-D with high time resolution.

In order to finely capture the trend of the water vapour absorption, the same measurement was performed using PBGF-D (55 m) but with much higher time resolution. Furthermore, the temperature behaviour of the water vapour was also recorded. The 55 m fibre sample was exposed to atmospheric conditions for 3 hours before both ends were sealed using the splicing process described above. Subsequently, water absorption spectra were recorded for 12 days at 22 °C and a further 12 days at 85 °C before the temperature was reduced again to 22 °C. Fig. 4 shows the evolution of absorption strength at 1369.85 nm during this time period. Day 0 corresponds to just after splicing. The water absorption strength decreased and approached the equilibrium state at 22 °C as observed in Fig. 3. When the sample was baked at 85 °C, the absorption quickly increased and then gradually decreased again. When the temperature returned to 22 °C, the absorption quickly reduced and did not show any further change. In addition, it was confirmed from the transmission at 1550nm during these measurements (Fig. 4) that the insertion loss did not significantly vary due to water vapour dynamics or temperature changes (a very small change in insertion loss ~0.07 dB occured when the temperature was returned to 22 °C). Here, there was no variable connection loss as all connections were fixed during the measurement. This result suggests that transmitted power at wavelengths away from water vapour absorption bands is not affected by the dynamics of water vapour.

The high-time resolution measurement indicates that the reduction of the water vapour absorption strength does not follow a simple exponential decay; in fact, initially there is an approximately linear trend. There are two possible explanations to the discontinuous point at day 1. Firstly, different reaction processes with the glass surface; chemi- and physi-sorption were observed in the adsorption kinetics of water vapour onto borosilicate glass surfaces[12]. Secondly, the

gas flow dynamics within the fibre; water molecules could be removed from the optical interaction path due to the combination of convection and diffusion of water vapour[13] along the fibre length in the hollow core. Through these processes, water vapour driven along the fibre length could move to regions with lower overlap with the optical path (e.g. near the inner surface) or with surfaces with a higher probability of reaction with the molecules.

The large jump of the absorption strength at the change to 85 ℃ suggests that the water vapour adsorbed on the inner glass surfaces prior to day 12 returned to the core region by desorption of physically adsorbed water molecules[11]. Prior to day 12, these water molecules existing on the surface would not be optically detectable due to the small overlap of the mode field with the glass. The desorbed water molecules would then be captured by other available sites on the silica surface during the high temperature period, which results in the subsequent reduction of the absorption strength. In addition the high absorption strength (~9 dB) observed at the change to 85 ℃ indicates that there had already been some water molecules adsorbed onto the inner glass surfaces prior to day 0, possibly originating from previous exposure to the atmosphere, because it surpassed that observed at day 0 by ~3 dB.

The reduction of the absorption strength at day 24 could be due to the adsorption-desorption process of water molecules. The physical reaction of water vapour with a silica surface is given by[11]:

$$\text{Si-OH} + \text{H}_2\text{O} \underset{k_{pd}(T)}{\overset{k_{pa}(T)}{\rightleftarrows}} \text{Si-OH} \ldots \text{OH}_2 \quad T \leq 400℃ \qquad (2)$$

$$\text{Si-O-Si} + \text{H}_2\text{O} \underset{k_{cd}(T)}{\overset{k_{ca}(T)}{\rightleftarrows}} 2 \cdot (\text{Si-OH}) \quad T > 400℃ \qquad (3)$$

where $k_{pa}(T)$ and $k_{pd}(T)$ are the physical adsorption and desorption rate coefficients, and $k_{ca}(T)$ and $k_{cd}(T)$ are the chemical adsorption and desorption rate coefficients, respectively. When the temperature returned to 22 ℃ in our sample, the physical coefficients adjusted to satisfy the new equilibrium state, which resulted in the quick reduction of the absorption strength.

III Conclusions

Water vapour has the potential to impact the optical properties in HCFs. In this study, water vapour absorption in HC-PBGFs was monitored to obtain insight into the behaviour of water molecule in HCFs. HC-PBGFs in an open condition showed an increase in water vapour absorption. This indicates that water vapour in the atmosphere diffuses into the hollow core. The diffusion rate varies between different fibre samples and due to changes in the surrounding environment. A reduction of water vapour absorption was observed in spliced HCFs and the hermetic condition suggests that some chemical and physical reactions occurred inside the HCFs between the confined water vapour and the silica glass surfaces. Although trends were consistent across a range of fibre samples, different rates of change of the water absorption were observed which could be linked to the condition of the silica surfaces and possibly the fibre length. No negative effects of these reactions (e.g. increased insertion loss from surface scattering) were observed as the transmitted power at 1550 nm did not significantly change at 22 ℃ or 85 ℃.

IV References

[1] Bradley, T. D., Hayes, J. R., Chen, Y., et al., "Record low-loss 1.3 dB/km data transmitting antiresonant hollow core fibre," Proc. Eur. Conf. on Optical Communication, Th3F: Post-deadline papers (2018).
[2] Wheeler, N. V., Petrovich, M. N., Baddela, N. K., et al., "Gas Absorption between 1.8 and 2.1 μm in Low Loss (5.2 dB/km) HC-PBGF," Proc. Conference on Lasers and Electro-Optics (CLEO), paper CM3N.5 (2012).
[3] Glaesemann, G. S., "Optical Fiber Mechanical Reliability Review of Research at Corning's Optical Fiber Strength laboratory," CORNING, 1-62 (2017).

[4] Hodgkinson, J. and Tatam, R. P., "Optical gas sensing: a review," Meas. Sci. Technol. 24, 012004, 1-59 (2013).
[5] Mousavi, S. A., Mulvad, H. C. H., Wheeler, N. V., et al., "Nonlinear dynamic of picosecond pulse propagation in atmospheric air-filled hollow core fibers," Optics Express 26(7), 8866-8882 (2018).
[6] Buric, M. P., Chen, K. P., Falk, J., et al, "Enhanced spontaneous Raman scattering and gas composition analysis using a photonic crystal fiber," Applied Optics 47(23), 4255-4261 (2008).
[7] Chen, Y., Wheeler, N. V., Baddela, N. K., et al., "Understanding Wavelength Scaling in 19-Cell Core," Proc. Optical Fiber Communication Conference, OSA Technical Digest (online) (Optical Society of America, 2014), paper M2F.4 (2014).
[8] Gris-Sánchez, I. and Knight, J.C., "Time-Dependent Degradation of Photonic Crystal Fiber Attenuation Around OH Absorption Wavelengths," Journal of Lightwave Technology 30(23), 3597–3602 (2012).
[9] Chen, Y., Liu, Z., Sandoghchi, S. R., et al., "Multi-kilometer Long, Longitudinally Uniform Hollow Core Photonic Bandgap Fibers for Broadband Low Latency Data Transmission," Journal of Lightwave Technology, 34(1), 104-113 (2016).
[10] Zeng, Q., Xu, S., "A two-parameter stretched exponential function for dynamic water vapor sorption of cement-based porous materials," Material and Structure 50, 128 (2017).
[11] Feng, A., Mccoy, B. J., Munir, Z. A., et al., "Water Adsorption and Desorption Kinetics on Silica Insulation," Colloid and Interface Science 180(1), 276-284 (1996).
[12] Tuzi, Y., "Sorption of Water Vapour on Glass Surface in Vacuum Apparatus," Journal of the Physical Society of Japan 17(1), 218-227 (1962).
[13] Masum, B. M., Aminossadati, S. M., Kizil, M. S., et al., "Numerical and experimental investigations of pressure-driven gas flow in hollow core photonic crystal fibers," Applied Optics 58(4), 963-972 (2019).